



Shear damage mechanism and early warning study of shale standard layer casing

Suling Wang¹, Xuefei Wang^{1,2}, Minzhan Chen¹, Kangxing Dong¹, Minzheng Jiang^{1*}, Lei Yang³

¹School of Mechanical Science and Engineering, Northeast Petroleum University, Daqing 163318, China

²School of Mechatronics Engineering, Qiqihar University, Qiqihar 161001, China

³Ningde Times New Energy Technology Co. Ltd. Ningde 352000, China

* Corresponding author: jmz1964@126.com

ABSTRACT

Aiming at the problem of shear-induced casing damage caused by standard layer shale soaking water, the theory of rock mechanics is used to establish the fluid-solid coupling calculation model of the formation-cement ring-casing of the standard interval shale interbed. It allows obtaining the strain and deformation changes of casing shear damage, and it puts forward the casing logarithmic strain exacerbated area should prompt adoption of reasonable measures to slow down the casing damage. Three-level orthogonal numerical simulation experiments were carried out for the five factors affecting casing damage. The simulation results show the critical strain data of the casing damage and the true strain data of the casing under the influence of five factors. According to the statistical principle, the predictive mathematical model of the critical strain and true strain prediction of the casing is obtained by the multiple regression method. The prediction of the strain state of the casing under actual working conditions is realized, and then the casing damage early warning was also realized.

Keywords: casing damage; shear deformation; numerical simulation; critical strain; early warning.

Mecanismo de daño por cizallamiento y estudio de alerta temprana de revestimiento de capa de lutita estándar

RESUMEN

Con el fin de abordar el problema del daño de la tubería de revestimiento inducido por el corte causado por el agua de remojo en capas de lutita estándar, la teoría de la mecánica de rocas se utiliza para establecer el modelo de cálculo de acoplamiento fluido-sólido de la envoltura de anillo de cemento de formación del intervalo estándar de esquistos intercalados. Esta permite obtener los cambios de tensión y de deformación del daño por cizalladura de la tubería de revestimiento, y presenta el área exacerbada por deformación logarítmica del revestimiento. También, debe impulsar la adopción de medidas razonables para reducir el daño de la tubería de revestimiento. En este trabajo se llevaron a cabo experimentos de simulación numérica ortogonal de tres niveles para los cinco factores que afectan el daño de la tubería. Los resultados de la simulación muestran los datos críticos de tensión del daño de la tubería y los datos reales de tensión de esta bajo la influencia de los cinco factores. De acuerdo con el principio estadístico, el modelo matemático predictivo de la deformación crítica y la predicción de deformación verdadera de la tubería se obtiene mediante el método de regresión múltiple. En este estudio se realiza la predicción del estado de deformación de la tubería de revestimiento en condiciones de trabajo reales y luego se analiza la alerta temprana en daños de la tubería.

Palabras clave: tubería de revestimiento; deformación por cizallamiento; simulación numérica; tensión crítica; alerta temprana.

Record

Manuscript received: 12/03/2019

Accepted for publication: 17/03/2020

How to cite item

Wang, S., Wang, X., Dong, K., Jiang, M., Chen, M., Xie, W., Zhang, Z., & Yang, L. (2020). Shear damage mechanism and early warning study of shale standard layer casing. *Earth Sciences Research Journal*, 24(2), 225-229. DOI: <https://doi.org/10.15446/esrj.v24n2.87932>

Introduction

By the end of 2016, the cumulative number of wells drilled in a certain area of Daqing Oilfield was 20,349, and the casing was damaged in 5,715 wells, accounting for 28.1% of the number of wells. Among them, the number of casing damage wells in a standard layer is 2325, accounting for 40.6% of the total number of casing damage wells. The casing damage in the non-oil layer is the most harmful to oilfield development. Data shows that the two peaks of the casing damage are concentrated in the standard layer shale parts. The casing damage wells continue to increase and have caused millions or even billions of economic losses to the oilfield. Therefore, prevention of casing damage is imminent.

The QRA method and LRFD method for reliability evaluation the strength of casing was proposed abroad in the early 1990s (Miller, 1998; Lewis, 1995). The method of risk and reliability evaluation is an important tool to solve the problem of uncertain factors in foreign drilling projects (Cunha et al., 2005). There are limited researches on domestic oil and water well casing damage warning (Hualin et al., 2010). Encheng Wu and Tie Yan broke through the viewpoint that casing damage is caused by oil shale swelling with water, and concluded that after the fossil layer enters the water, under the action of fluid pressure and ground stress, when the shear stress exceeds the shear strength of the weak surface of the fossil layer, the formation becomes unstable and the sheet casing damage occurs (Encheng & Tie, 2007). Lianping Li pointed out that the standard layer casing damage is the result of mechanical shearing. Shear damage is the main form of casing damage and there is a casing damage shear zone (Lianping, 2007). Chi Ai et al analyzed the influence of casing steel grade and wall thickness on the critical condition of casing damage. He analyzed the main factors influencing the critical slip of casing from the angle of delaying the shear damage of casing (Chi et al., 2015). Yanjun Zhou et al proposed a dynamic prediction method for causing damage based on the integration of rough sets and support vector machines (Zhou et al., 2010). Guorong Wang et al obtained the prediction model of casing reliability life by qualitative and quantitative analysis of casing fault tree, and deduced the calculation formula of the upper and lower limit of casing damage in a period of time after completion (Guorong et al., 2002).

In order to solve the problem of large number of casing damage in the standard layer of Daqing Oilfield, this study applied on-site oil well test data and numerical simulation data for comparison, the data are in good agreement that the simulation model is available. The key factors affecting casing damage are formation elastic modulus, the formation thickness, the formation dip angle, casing strength and water injection pressure. Three orthogonal tests were carried out on five factors. Numerical simulations were carried out to obtain critical strain data and casing true strain data. The multivariate regression method is used to obtain the prediction equation of the critical strain of the casing and the true strain of the casing, and the prediction method of casing damage based on the parameters of the well and the production parameters is obtained.

Establishment of standard layer formation-cement ring-casing numerical model

Through the analysis of the lithological characteristics of the bottom of a standard layer in Daqing oilfield, rock formation sampling is shown in Fig. 1. The rock mass at the bottom of this section belongs to typical jointed rock mass, and there are abundant bedding joints and micro-cracks. This structure facilitates rapid immersion of injected water, forming an expanding flooded area, when the submerged area is squeezed by external force, the rock mass will easily slip along the structural plane of the rock mass.

Taking the standard layer as the research object, establish a three-dimensional fluid-solid coupling mechanical model of the casing-cement ring-formation. Formation thickness and formation inclination are determined according to well conditions, the reservoir rock mass is subjected to the pressure of the overlying rock and the weight of the rock itself and the pressure of the production fluid in the casing (Wan Mahari et al., 2018). The initial osmotic pressure is applied to the upper, lower and circumferential surfaces of the formation, a fixed constraint is applied on the bottom surface, displacement constraints in the X and Y directions were applied to the outer surface to simulate the lateral constraint of surrounding formation rocks on the model, the mechanical model is shown in Fig. 2.



Figure 1. A sampling of a standard layer shale in Daqing Oilfield

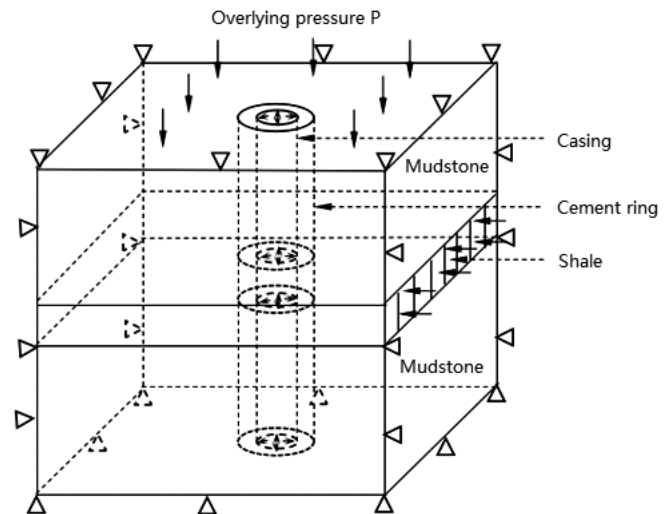


Figure 2. Standard layer casing damage analysis mechanical model

Considering the non-uniformity of the formation and the casing, the numerical model is used to calculate the above mechanical model, and the deformation and strain law of the casing under different formation conditions are obtained. The finite element model is shown in Figure 3.

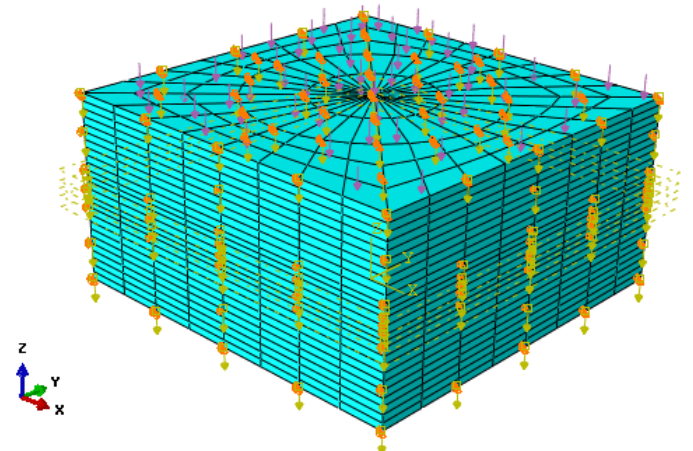


Figure 3. Standard layer casing damage analysis finite element model

According to the test data of a rock layer in Daqing Oilfield, set the rock formation of mudstone - shale - mudstone interbed structure, the upper and lower mudstones is set as creep materials, shale set into joint material (Cheng et al., 2019). Analysis under the condition of water immersion, due to the difference in mechanical properties between the layers, the deformation of the joint of the cementation position is uncoordinated and the casing deformation is damaged.

Joint materials include joint system water invasion and failure behavior, as well as the failure mechanism of matrix materials. The plastic behavior of the matrix material follows the linear Drucker-Prager failure criterion, and the joint material model uses the stress-based fracture opening criterion. When the crack is open, the model follows:

$$\varepsilon_{an(ps)}^{el} \leq \varepsilon_{an}^{el} \quad (1)$$

In the formula, ε_{an}^{el} is the normal elastic strain component across the crack, $\varepsilon_{an(ps)}^{el}$ is calculated from the plane stress assumption to calculate the normal elastic strain across the crack.

$$\varepsilon_{an(ps)}^{el} = -\frac{\nu}{E}(\sigma_{a1} + \sigma_{a2}) \quad (2)$$

In the formula, E is the elastic modulus of the material, ν is the Poisson's ratio, σ_{a1}, σ_{a2} is the radial stress on the joint surface. The sliding failure surface of the joint system a is defined as follows:

$$f_a = \tau_a - p_a \tan \beta_a - d_a = 0 \quad (3)$$

In the formula, β_a is the internal friction angle of the joint system a, d_a is the viscous force of the joint system a, τ_a is the shear stress on the joint surface, p_a is the vertical stress acting on the joint surface.

When $f_a < 0$, the joint system a does not slip. When $f_a = 0$, the joint system from sliding.

In the calculation process, the casing deformation is caused by the deformation of the standard layer. In order to accurately simulate the deformation state of the standard layer after water inflow, the simulation of the deformation of the casing is performed in two steps (Giwa et al., 2016). In the first step, the internal stress of the casing and the stress field of the formation caused by the cementing process are applied to the calculation model, and the initial geostress field of the casing-cement ring-formation model is simulated, in the second step, the water pressure boundary conditions are applied to the calculation model to simulate the shale water immersion process, and the casing strain and deformation law under different influent strengths are simulated to provide a basis for the casing damage determination.

Strain and deformation of the casing

This study selected a well in Daqing Oilfield for testing, the shale layer is located 923 meters underground and the shale thickness is 2.6 meters, the principal stresses in the three directions of X, Y and Z are 23.32 MPa, 22.25 MPa and 25.16 MPa the dip angle of the formation is about 3 degrees, the casing diameter is 51/2", and the yield limit of the casing is 552 MPa. In the field logging process, the well detection uses continuous monitoring and stores test data, and continuously monitors for 9 months, as shown in Fig. 4. According to the above theory and data, the strain of the casing is obtained



Figure 4. Oilfield oil well test

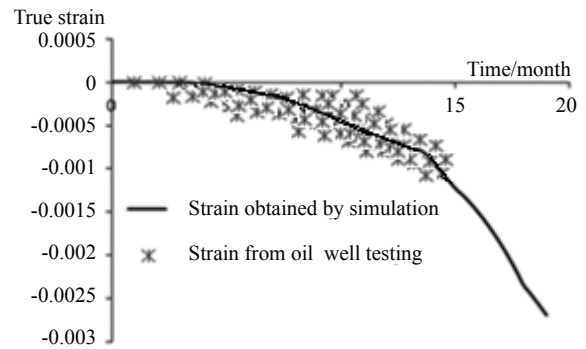


Figure 5. Comparison of monitoring and calculation of logarithmic strain outside the casing

by simulation, as shown in Fig. 5, casing strain value detected by the oil well and the casing strain value calculated by simulation. It can be observed in the figure that the oil well test strain data and simulation results are consistent, indicating the correctness of the calculation model and method.

The Outer load of the casing is 20 MPa, 30M Pa, 40 MPa, 50 MPa respectively. The strain and deformation of the simulated casing change with time, as shown in the casing strain cloud diagram of Fig. 6, the bending deformation position of the casing is the concentration region of plastic strain.

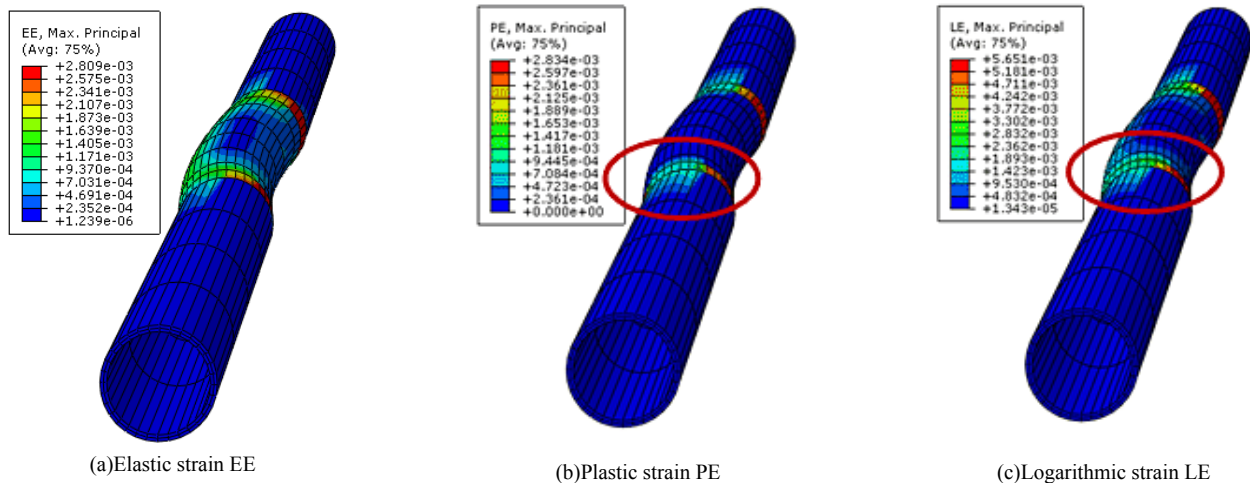


Figure 6. Casing strain cloud

The true strain is defined as the natural logarithm of the ratio of the current length of the initial length, so it is also called logarithmic strain, which is a combination of elastic strain and plastic strain. The elastic strain, plastic strain and true strain in the bending position of the casing is extracted, Figure 7 shows the variation of the elastic strain and plastic strain of the casing with time under different loads:

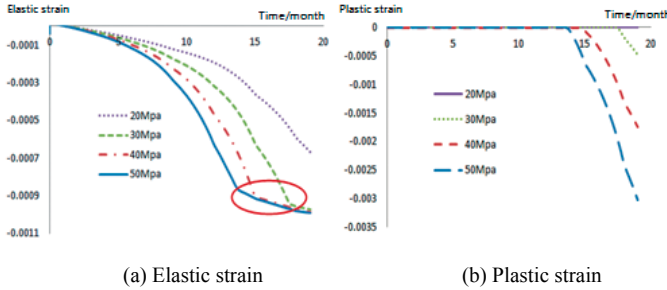


Figure 7. Variation of elastic strain of casing with time under different loads

When the water injection pressure outside the casing is faster or the pressure outside the casing is larger, the critical elastic strain of the casing gradually decreases with the increase of the external pressure of the casing. But the reduction is small, and the external load is 40 MPa compared with 50 MPa when the plastic deformation occurs. The difference of the elastic strain of the casing is 0.00003, which is about 3.5%, after the casing reaches the plastic deformation, the elastic strain of the casing increases slowly, and the rate of elastic strain of the casing under different external pressures is the same. With the extension of time, the elastic deformation of the casing is basically the same. The larger the external load is, the earlier the deformation will be. The plastic strain rate of the casing is not affected by external pressure. Since field detection shows the comprehensive strain of elastic strain and plastic strain, the variation law of logarithmic strain is extracted, as shown in Figure 8.

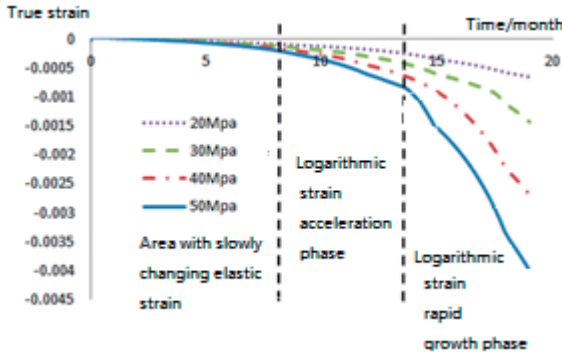


Figure 8. Horizontal logarithmic strains of casing under different loads

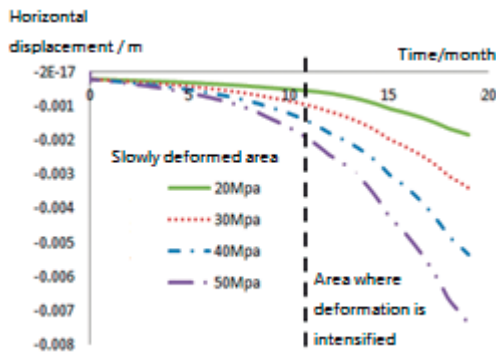


Figure 9. Horizontal deformations of the casing under different loads

Figure 8 shows the horizontal logarithmic strain of casing under different loads. The strain growth curve can be divided into the logarithmic strain slow growth phase, the accelerated growth phase and the rapid growth phase. The casing deformation law corresponding to Fig. 9 is the slow deformation phase and the deformation acceleration phase. The slow growth phase of logarithmic strain mainly occurs in the initial stage of elastic deformation of casing, and the acceleration phase of logarithmic strain is the stage of elastic instability of casing, and the stage of rapid growth is the stage of plastic strain of casing. In the elastic instability stage and the plastic deformation stage, the casing deformation is in the acceleration zone, which is the instability zone of the casing deformation, and the casing damage is intensified at this stage. When the elastic strain of the casing accumulates to a certain extent, the plastic strain increases sharply and the casing enters the plastic strain phase. From the point of view of the management of casing damage, in the accelerated growth phase of casing logarithmic strain, timely take appropriate measures to slow the casing damage.

This study proposes a method to predict the critical strain and the true strain of the casing. When the true strain of the casing exceeds the critical strain of the casing, the casing will enter the plastic deformation stage and an early warning to reduce casing damage.

Standard layers casing loss prediction

The main factors affecting the casing include: formation elastic modulus, formation thickness, formation inclination, casing strength and water injection pressure. This study conducts 3 level orthogonal tests on 5 parameters, according to the numerical simulation method established above, the true strain value of the casing and the critical strain value when the casing is damaged are obtained, the calculation results are shown in Fig. 10.

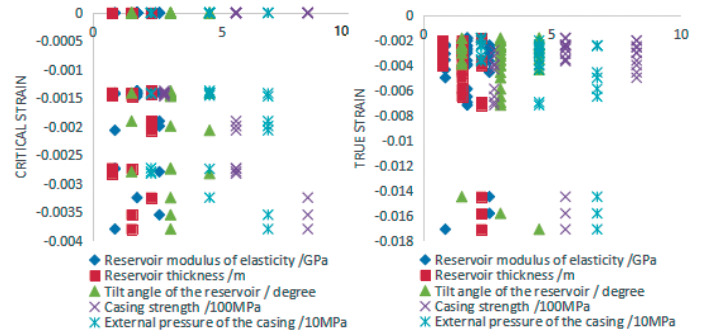


Figure 10. Orthogonal test numerical simulation results data scatter plot

It is concluded from Figure 10 that the three levels of the reservoir elastic modulus, reservoir thickness, reservoir angle, casing strength and casing water injection pressure are combined to obtain 37 sets of parameters and corresponding casing damage critical strain values and true strain value of the casing. The data analysis software was used to obtain the binary multiple regression equations which characterize the relationship between the critical strain and true strain and the above five factors, and the variance analysis method was used to verify the rationality of the equation. The equation was used to predict the casing damage. Then get the following mathematical model.

$$\varepsilon_{ij} = 8.4 \cdot 10^{-7} - 3.3 \cdot x_1 \cdot 10^{-5} - 3 \cdot x_2 \cdot 10^{-4} - 2.8 \cdot x_3 \cdot 10^{-6} - 3.9 \cdot x_4 \cdot 10^{-6} + 3.9 \cdot x_4 \cdot 10^{-6} + 3.05 \cdot x_5 \cdot 10^{-3} \quad (4)$$

$$\varepsilon_{zs} = 62 + 37 \cdot x_1 - 82 \cdot x_2 + 30 \cdot x_3 - 3.5 \cdot x_4 \cdot 10^{-2} - 2.7 \cdot x_5 - 7.3 \cdot x_1^2 + 22 \cdot x_2 + x_3^2 + 6.8 \cdot x_4 \cdot 10^{-5} + 2.3 \cdot x_5^2 \cdot 10^{-2} - 2.4 \cdot x_1 \cdot x_2 + 4.1 \cdot x_1 \cdot x_3 \cdot 10^{-2} + 2.4 \cdot x_1 \cdot x_4 \cdot 10^{-4} - 15 \cdot x_1 \cdot x_5 \cdot 10^{-1} - 1.1 \cdot x_2 \cdot x_3 - 2.9 \cdot x_2 \cdot x_4 \cdot 10^{-2} + 1.9 \cdot x_2 \cdot x_5 - 2.8 \cdot x_3 \cdot x_4 \cdot 10^{-3} - 3.9 \cdot x_3 \cdot x_5 \cdot 10^{-1} - 3.4 \cdot x_4 \cdot x_5 \cdot 10^{-4} \quad (5)$$

Among them, ε_{ij} is the casing critical strain; ε_{zx} is the casing true strain; x_1 is the reservoir elastic modulus, GPa; x_2 is the reservoir thickness, m; x_3 is the reservoir inclination, degree; x_4 is the casing strength, MPa; and x_5 is the outer casing pressure, MPa.

Comparing the measured critical strain and true strain curve with the multiple regression fitting theoretical curve by comparing Fig. 11 with Fig. 12, it can be seen that the formula of multiple regression theory can fit the sample data well.

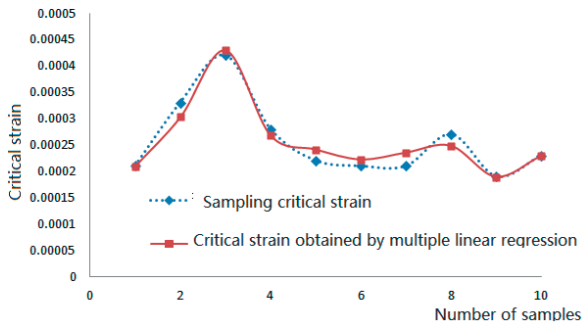


Figure 11. Comparison of Sampling Critical Strain Data and Multiple Regression Critical Strain Curves

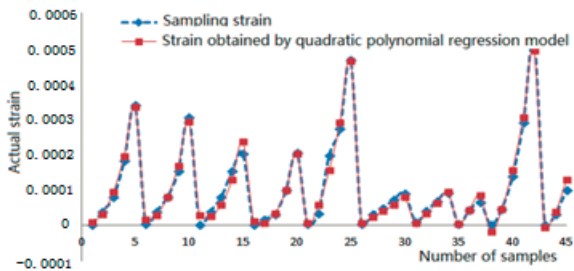


Figure 12. Comparison of on-site sampling data with theoretical curves

According to the prediction equations of critical strain and true strain of the casing obtained by binary regression, the critical strain value of the casing and the true strain of the casing can be predicted under conditions of known oil well parameters and production parameters. The equation is

$$\varepsilon_{zs} \geq \varepsilon_{lj} \quad (6)$$

If the equation (6) is satisfied, the casing begins to undergo unstable deformation and enters the stage of plastic deformation, and measures need to be taken in time, otherwise, the casing is stable and no instability damage occurs. The prediction equation is suitable for the standard layer of the second section of Daqing Oilfield. Other oilfields can use the above method to determine the prediction equation and to determine the damage of the casing.

Conclusion

(1) The main cause of casing shear damage is the slippage of the standard shale layer. According to the theory of rock mechanics, creeping materials are utilized to the upper and lower mudstones, and joint materials are used for shale. The fluid-solid coupling calculation model of the formation-cement ring-casing of the standard interval mudstone shale interbed is established, and the deformation low of casing shear damage is obtained. The simulation results are compared with actual logging results of Daqing Oilfield, the rationality of the numerical model is verified and a simulation method of standard casing damage is proposed.

(2) In the shear damage process, the transition from elastic strain to plastic strain is the initial stage of casing damage. From the perspective of casing damage prevention, steps taken to reduce casing damage should be taken during the casing strain acceleration phase. Built on the above theory, this study proposes a method for predicting the true strain and critical strain.

(3) The five factors affecting casing damage are casing strength, rock inclination, rock thickness, rock elastic modulus, and external load. The five factors were divided into three levels for orthogonal numerical simulation experiments, and data on the correlation between the five factors and the critical strain and true strain of the casing were extracted. According to the statistical principle, the multivariate regression method is used to obtain the mathematical model of the critical strain and true strain prediction of the casing. When the true strain exceeds the critical strain, the casing deformation enters the plastic phase and the casing damage occurs. The prediction of the strain state of the casing under actual working conditions is realized according to the formation parameters and logging data, which provide a new method for preventing casing damage.

(4) The theoretical formula for the shear damage of the standard layer casing of the Nen 2 section of Daqing Oilfield has certain practicability.

Acknowledgments

This research was supported by Cooperation project between Heilongjiang Province and academicians (2019sy0304) and China Postdoctoral Science Foundation(2019M661249). The authors would like to thank Daqing Oilfield for providing data on sampling stress and strain.

References

- Cheng Y. W., Ng, K. H., Lam, S. S., Lim, J. W., Wongsakulphasatch, S., Witoon, T., & Cheng, C. K. (2019). Syngas from catalytic steam reforming of palm oil mill effluent: An optimization study. *International Journal of Hydrogen Energy*, 44(18), 9220-9236.
- Chi, A., Chaoyang, H., & Yueming, C. (2015). Casing optimization for delaying standard Layer damage of Daqing Oilfield. *Petroleum Drilling Techniques*, 43(06), 7-12.
- Cunha, J. C., Demirdal, B., & Gui, P. (2005). *Use of quantitative risk analysis for uncertainty quantification on drilling operations-review and lessons learned*. Society of Petroleum Engineers, 94980.
- Encheng, W., & Tie, Y. (2007). Analysis of the mechanism of casing damage caused by the standard layer of fossil layer in the Second Layer of Daqing Oilfield. *Journal of Daqing Petroleum Institute*, (02), 38-41+125.
- Giwa, S. O., Adama, K. O., Nwaokocha, C. N., & Solana, O. I. (2016). Characterization and flow behaviour of sandbox (*Hura crepitans* Linn) seed oil and its methyl esters. *International Energy Journal*, 16(2), 65-72.
- Guorong, W., Qingyou, L., & Xia, H. (2002). Prediction of casing reliability life. *Natural Gas Industry*, 22(5), 53-55.
- Hualin, L., Zhichuan, G., Zhenlai, Y., & Guangjun, M. (2010). A risk assessment method for casing failure based on reliability theory. *Acta Petrolei Sinica*, 31(01), 161-164+172.
- Lewis, D. B. (1995). *Load and resistance factor design for oil country tubular goods*. Offshore Technology Conference, 7936.
- Lianping, L., Hongqing, K., Guizhen, J., Qin, L., & Qing, Liu. (2007). A new understanding of the formation mechanism of casing damage in Xingbei Development Zone and the comprehensive prevention and control technology of casing damage. *Daqing Petroleum Geology and Development*, (01), 83-87.
- Miller, R. A. (1998). *Real world implementation of QRA methods in casing design*. Society of Petroleum Engineers, 48325.
- Wan Mahari, W. A., Chong, C. T., Cheng, C. K., Lee, C. L., Hendrata, K., Yek, P. N. Y., Ma, N. L., & Lam, S. S. (2018). Production of value-added liquid fuel via microwave co-pyrolysis of used frying oil and plastic waste. *Energy*, 162, 309-317.
- Zhou, Y., Jia, J., & Li, R. (2010). A dynamic prediction method for casing damage based on rough set theory and support vector machine. *Journal of China University of Petroleum (Natural Science Edition)*, 34(06), 71-75.

